DOI: 10.61782/fa.2023.0558

forum acusticum 2023

ELECTRO-ACTIVE ACOUSTIC LINER FOR THE REDUCTION OF TURBOFAN NOISE

Édouard Salze[1*] **Emanuele de Bono**[2] **Kévin Billon**[3] **Martin Gillet**[2]
Maxime Volery[4] **Manuel Collet**[3] **Morvan Ouisse**[2] **Hervé Lissek**[4] **Jacky Mardjono**[5]
[1] Univ. Lyon, École Centrale de Lyon, LMFA UMR CNRS 5509, Écully, France
[2] SUPMICROTECH, Université de Franche-Comté, CNRS, Institut FEMTO-ST, Besançon, France
[3] Univ. Lyon, École Centrale de Lyon, LTDS UMR 5513, Écully, France
[4] École Polytechnique Fédérale de Lausanne, LTS2, Switzerland
[5] Safran Aircraft Engines, Moissy-Cramayel, France

ABSTRACT

An electro-active acoustic liner is used to lower the noise emissions of a turbofan engine. The liner is composed of an array of electro-acoustic absorbers, covered by a wiremesh in order to protect the electrodynamic devices from the flow. The electro-active liner is operated using a pressure-based and current-driven control architecture, for the synthesis of specific acoustic impedances. Experiments are performed in the PHARE-2 test-rig at École Centrale de Lyon, representative of a real turbofan engine at the laboratory scale. The obtained results underline the efficiency of the proposed concept on both tonal and broadband noise for a large range of operating points of the turbofan engine, including transsonic conditions.

Keywords: *active liner, UHBR engine, modal decomposition*

1. INTRODUCTION

With the new generation of aircraft engines exhibiting ultra high by-pass ratios (UHBR), reducing fuel consumption and noise emissions are two of the main design objectives. UHBR engines exhibit shorter nacelles and a lower frequency content, because of the reduced rotational speed of the fan. The performances of conventional acoustic inlet liners are then expected to drop, as less surface is available. In that context, active liners should achieve higher noise reduction with limited surface, and in particular break the quarter wavelength limitations of conventional honeycomb liners.

*__Corresponding author__: edouard.salze@ec-lyon.fr.

2. EXPERIMENTAL SET-UP

2.1 The ECL-B3 (PHARE-2) test-rig

The ECL-B3 test-rig is located at École Centrale de Lyon, LMFA, inside an anechoic chamber. The rotational speed, up to 16 000 rotations per minute, is provided by a 3 MW electrical engine. The air flow, up to about 40 kg.s^{-1}, generated by the turbofan, passes through acoustic baffles on the roof of the building. Using this test-rig, interest was focused on the characterization of UHBR industrial turbofans, regarding acoustic aspects [9], modal decomposition [6], and aerodynamic instabilities [3]. Current and future test campaigns are dedicated to the realization of an academic open test-case [2, 5, 8].

The experimental configuration is sketched in Figure 1. The electro-active liner is located in the inlet of the test-rig at the location marked in red in Figure 1. The data analyzed in the present paper is obtained from two microphone rings, upstream and downstream of the liner, with 9 and 7 microphones respectively, as depicted in Figure 1. Acoustic radiation of the test-rig is also measured using an external microphone array.

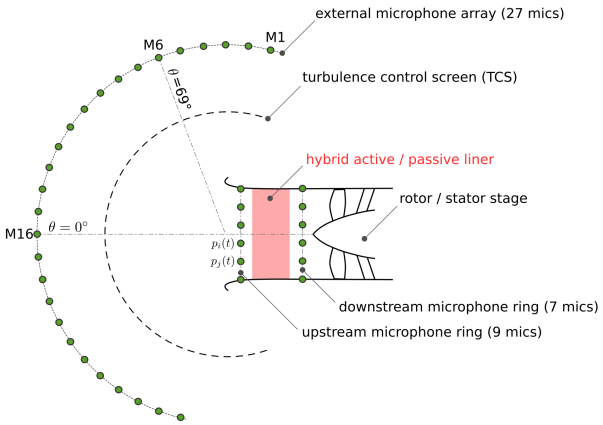

Figure 1. Microphone arrays for the extraction of the liner efficiency: external microphone array with 27 microphones, upstream microphone ring with 9 microphones, and downstream microphone ring with 7 microphones.

2.2 Experimental data processing

All microphone signals are synchronously sampled during 1 min at 102.4 kHz, using blocks of 1 s with a 50% overlap. The cross-power spectral density between two pressure signals $p_i(\mathbf{x}_i, t)$, $p_j(\mathbf{x}_j, t)$, noted S_{ij} in this paper, is computed as

$$S_{\text{ij}}(\mathbf{x}, \mathbf{r}, \omega) = 2\pi E\left[\hat{p}_i(\mathbf{x}_i, \omega)\hat{p}_j^*(\mathbf{x}_j, \omega)\right]$$

The liner efficiency is expressed as an Insertion Loss (IL), compared to a reference configuration, as

$$IL(\mathbf{x}_i, \tilde{f}) = S_{\text{ii}}^{\text{ref}}(\mathbf{x}_i, \tilde{f}) - S_{\text{ii}}(\mathbf{x}_i, \tilde{f})$$

where $\tilde{f}$ denotes the frequency axis, normalized to the frequency rotation of the shaft, also called the *engine order*.

2.3 Active liner implementation

The objective of the implementation is to synthesize a target impedance. As sketched in Figure 2, each cell uses a loudspeaker, four microphones at the corners, and an electronic card (not represented in Figure 2). The liner is assembled using a total of 56 cells, arranged in a two rows configuration.

Each loudspeaker membrane is driven as a function of the wall-pressure measurement [7]. The equation driving

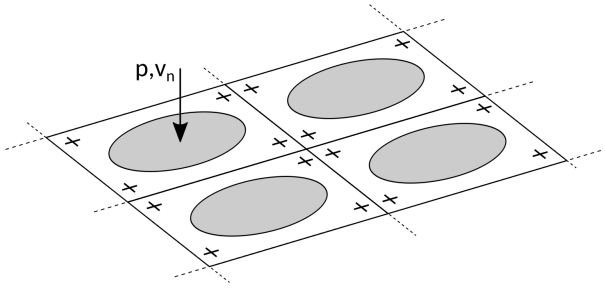

Figure 2. Sketch of the active liner as an array of individual square active cells. Each cell uses a loudspeaker and four microphones, located at the corners.

the loudspeaker in a single degree of freedom piston mode can be written as

$$Z_m(s)v_n(s) = S_d p(s) - B\ell i(s)$$

where s stands for the Laplace variable, $v_n(s)$ is the membrane normal velocity of the loudspeaker, $p(s)$ the wall-pressure fluctuations, S_d the equivalent piston area, $B\ell$ the force factor of the moving coil and $i(s)$ is the coil electrical current. In this paper, the wall-pressure fluctuations $p(s)$ are averaged over the four microphones for each cell. Alternatively, the control strategy can be based on the pressure gradient estimation over microphone pairs. This approach will be presented later in another communication. To achieve the targeted impedance Z_{at} at the surface, the transfer function between $p(s)$ and $i(s)$ is defined as

$$H_{loc}(s) = \frac{i(s)}{p(s)} = \frac{1}{B\ell}\left(S_d - \frac{Z_m(s)}{Z_{at}(s)}\right),$$

The target impedance Z_{at}, as a function of the acoustic resistance R_{at} at the loudspeaker resonance, is

$$Z_{at}(s) = \frac{p(s)}{v_n(s)} = \mu_1 \frac{sM}{S_d} + R_{at} + \mu_2 \frac{1}{sCS_d},$$

The parameters μ_1 and μ_2 represent the mass and stiffness of the controlled loudspeaker, respectively. By tuning those two parameters, the active liner can be adapted to different frequency bands.

3. RESULTS AND DISCUSSION

Interest is focused on two operating conditions of the test-rig: operating point 1 (OP1) at 30% of the test-rig nominal

rotational speed, around $N = 3500$ rotations per minute, and operating point 2 (OP2), at the nominal rotational speed, around $N = 12000$ rotations per minute. At 30% of the test-rig nominal rotational speed, the active liner is set to target the blade passing frequency of the rotor at $\tilde{f} = 16$. At 100% of the test-rig nominal rotational speed, the parameters are set to target low-frequency tonal components $\tilde{f} = 3$ and 4. The list of operating points and the associated control parameters are indicated in Table 1.

Op. point	N (%)	μ_M	μ_K	R_{at}/Z_0
OP1-a	30	0.3	0.7	1
OP1-b	30	0.3	1	2.5
OP1-c	30	0.5	1.26	0.75
OP2-a	100	0.5	0.479	0.15
OP2-b	100	0.5	1.33	1

Table 1. Operating points analyzed in the present paper, with the associated control parameter μ_M, μ_K and R_{at}

At 30% of the nominal rotational speed, the radiated noise exhibit two components : a broadband contribution and a tonal component located at the blade passing frequency $\tilde{f} = 16$. An attenuation of around 6 dB is obtained at the blade passing frequency. The passive contribution of the liner is around 2 dB at the tone. The broadband attenuation of the electro-active liner is visible on the third-octave bands spectra in Figure 3 for operating point OP1-c. A passive broadband contribution (in black) of 3 to 4 dB is obtained for $\tilde{f} > 10$, approximately. Below $\tilde{f} = 10$, the acoustic wavelength is approximately ten times larger than the depth of the cavity, therefore the passive efficiency is considerably reduced in the low-frequencies. An active contribution of around 2 dB of the liner is obtained (in grey in Figure 3).

The insertion loss (IL) is indicated in Figure 4 at 30% of the nominal rotational speed (see Table 1). The maximum attenuation of 6 dB at $\tilde{f} = 16$ is obtained with the lowest acoustic resistance R_{at} (operating point OP1-c with $R_{at}/Z_0 = 0.75$). However, a larger bandwidth is obtained when reducing the μ_K parameter at operating point OP1-a, at which a higher attenuation up to 5 dB is obtained below $\tilde{f} = 16$.

At 100% of the nominal rotational speed, additional tonal components below the blade passing frequency are obtained. At transsonic conditions, shockwaves are emitted at the tips of the blades, leading to a reinforcement

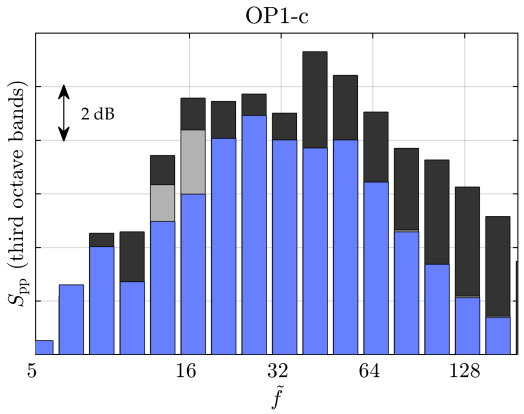

Figure 3. Power density spectra S_{pp} in third-octave bands, measured at $\theta = 69°$ (microphone 6, see Figure 1), as a function of engine order $\tilde{f}$: no liner (rigid turbofan inlet), active liner switched off, active liner at operating point *OP1-c*.

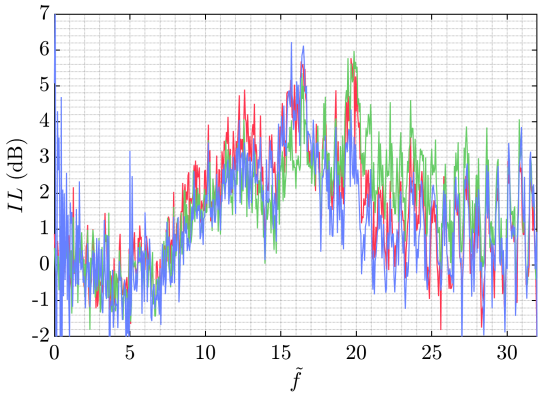

Figure 4. Insertion Loss (IL), as a function of engine order $\tilde{f}$: operating point *OP1-a*, operating point *OP1-b*, operating point *OP1-c*.

of harmonics of the shaft frequency at each integer values of the engine order $\tilde{f}$. The insertion loss obtained is indicated in figure 5. The third harmonic of the shaft ($\tilde{f}$=3, operating point OP2-a) could be attenuated of about 10 dB, whereas different parameters of the liner enabled an attenuation of 11 dB of the fourth harmonic, which demon-

strates the ability of the liner to reach different frequency contents.

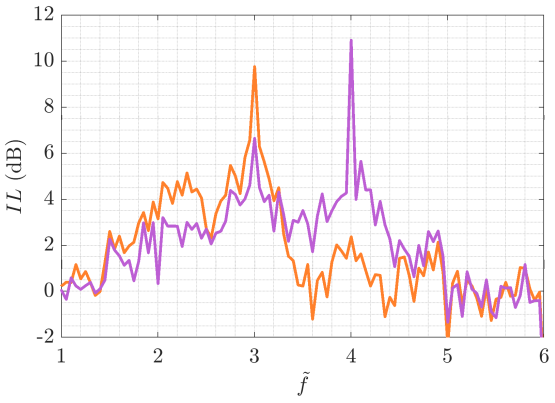

Figure 5. Insertion Loss (IL), as a function of engine order $\tilde{f}$: —— operating point *OP2-a*, —— operating point *OP2-b*

4. CONCLUSION

An electro-active liner is installed in the inlet of a turbofan engine, at a 1:4 laboratory-scale. An attenuation of 6 dB could be obtained at the blade passing frequency of a subsonic fan, combined with a broadband attenuation over a large frequency band. The ability to operate the liner on a transsonic fan was also demonstrated, with an attenuation of more than 10 dB of the harmonics of the shaft rotation. The ability to tune the liner to target different components opens the possibility to adapt to different rotational speeds, and therefore different cruise conditions.

5. ACKNOWLEDGMENTS

The authors are particularly grateful to Benoît Paoletti, Cédric Desbois and Antonio Pereira for their help in setting up and conducting the experiment. The present work has received funding from the Clean Sky 2 Joint Undertaking under the European Union's Horizon 2020 program SALUTE, under grant agreement N° 821093.

6. REFERENCES

[1] K. Billon, E. De Bono, M. Perez, E. Salze, G. Matten, M. Gillet, M. Ouisse, M. Volery, H. Lissek, J. Mardjono, M. Collet, "In flow acoustic characterisation of a 2D active liner with local and non local strategies", *Applied Acoustics*, **191**:108655, 2022. https://doi.org/10.1016/j.apacoust.2022.108655

[2] C. Brandstetter, V. Pages, P. Duquesne, B. Paoletti, S. Aubert, X. Ottavy, "Project PHARE-2— a high-speed UHBR fan test facility for a new open-test case.", *J. Turbomach.*, **141**(10): 101004, 2019. https://doi.org/10.1115/1.4043883

[3] C. Brandstetter, B. Paoletti, X. Ottavy, "Compressible Modal Instability Onset in an Aerodynamically Mistuned Transonic Fan", *ASME. J. Turbomach*, **141**(3):031004, 2019. https://doi.org/10.1115/1.4042310

[4] M. Munjal, *Acoustics of ducts and mufflers with application to exhaust and ventilation system design*, Wiley-Interscience publication, Wiley, 1987.

[5] V. Pagès, P. Duquesne, S. Aubert, L. Blanc, P. Ferrand, X. Ottavy, C. Brandstetter, "UHBR Open-Test-Case Fan ECL5/CATANA", *Int. J. of Turbomachinery, Propulsion and Power*, **7**(2):17, 2022. https://doi.org/10.3390/ijtpp7020017

[6] A. Pereira, E. Salze, J. Regnard, F. Gea-Aguilera, M. Gruber, "New modular fan rig for advanced aeroacoustic tests - Modal decomposition on a 20" UHBR fan stage", AIAA 2019-2604. 25th AIAA/CEAS Aeroacoustics Conference, 2019. https://doi.org/10.2514/6.2019-2604

[7] E. Rivet, S. Karkar, H. Lissek, "Broadband low-frequency electroacoustic absorbers through hybrid sensor-/shunt-based impedance control", *IEEE T. Contr. Syst. T.* **25**(1), pp 63-72, 2016. https://doi.org/10.1109/TCST.2016.2547981

[8] M. Rodrigues, L. Soulat, B. Paoletti, X. Ottavy, C. Brandstetter, "Aerodynamic investigation of a composite low-speed fan for UHBR application", *J. Turbomach.* **143**(10):101004, 2021. https://doi.org/10.1115/1.4050671

[9] E. Salze, A. Pereira, P. Souchotte, J. Regnard, F. Gea-Aguilera, M. Gruber, "New modular fan rig for advanced aeroacoustic tests - Acoustic characterization of the facility", AIAA 2019-2603. 25th AIAA/CEAS Aeroacoustics Conference, 2019. https://doi.org/10.2514/6.2019-2603